

## H<sub>2</sub> Production in the Radiolysis of Water on CeO<sub>2</sub> and ZrO<sub>2</sub>

Jay A. LaVerne\*,† and Lav Tandon‡

Radiation Laboratory, University of Notre Dame, Notre Dame, Indiana 46556, and  
Chemistry Division, Los Alamos National Laboratory, Los Alamos, New Mexico 87545

Received: August 8, 2001; In Final Form: October 17, 2001

The production of H<sub>2</sub> in the radiolysis of water adsorbed on micron-sized particles of CeO<sub>2</sub> and ZrO<sub>2</sub> has been examined. Radiation chemical yields of H<sub>2</sub> increase substantially with decreasing number of adsorbed water layers when the yield is determined with respect to the energy deposited directly by  $\gamma$ -rays to the water. These yields reached values of 20 and 150 molecules of H<sub>2</sub> per 100 eV for one to two water layers on CeO<sub>2</sub> and ZrO<sub>2</sub>, respectively, compared to 0.45 molecule/100 eV in bulk liquid water. The yields of H<sub>2</sub> determined with respect to the total energy deposited in both the oxide and water were found to have a smaller, but observable, dependence on the amount of water adsorbed. Radiolysis of ZrO<sub>2</sub> with  $\gamma$ -rays produced about 5 times more H<sub>2</sub> than CeO<sub>2</sub> for the equivalent amount of water adsorbed. The results suggest that the increase in H<sub>2</sub> production is due to the transfer of energy, possibly by an exciton, from the oxide to the water. O<sub>2</sub> production was at least an order of magnitude less than H<sub>2</sub>. The yield of H<sub>2</sub> in the 5 MeV helium ion radiolysis of water on CeO<sub>2</sub> is the same as with  $\gamma$ -rays, but the results with ZrO<sub>2</sub> are substantially lower. The H<sub>2</sub> yields with helium ion radiolysis may be nearly independent of the type of oxide.

### Introduction

Understanding the radiolytic decomposition of water adsorbed on oxide surfaces involves a number of challenging aspects not normally encountered in radiation chemistry studies. One of the fundamental problems is to determine if the radiation-induced decomposition of water is different for molecules adsorbed on surfaces as compared to those in the bulk. The presence of a surface could lead to catalytic, steric, or other effects that alter the water decomposition. There is also the heterogeneous nature of the energy deposition since energy can migrate between the solid phase and the water to enhance or hinder water decomposition. This latter phenomenon can lead to problems in determining the “effective” dosimetry, which is equivalent to the amount of energy available for radiation effects in the adsorbed water. One would like to know the variation in products and their yields for adsorbed water as compared to bulk in order to determine the heterogeneous effects of radiolysis. There are also a number of very important practical reasons for radiolysis studies on adsorbed water. Water is in intimate contact with solid surfaces in the radiation fields of nuclear reactors and of wet nuclear waste materials in stainless steel storage containers. Variations in the yields of the potentially explosive product H<sub>2</sub> (or the ratio of H<sub>2</sub> to O<sub>2</sub>) or of the corrosive product H<sub>2</sub>O<sub>2</sub> can lead to significant management problems.

It appears that the first studies on the radiolysis of compounds in the absorbed state examined the decomposition of organics on a variety of mineral solids, especially silica gel. In general, the decomposition of the organics is enhanced in the adsorbed state as compared to the liquid or gas state. Allen and co-workers attributed the increase in radiolytic yields to an energy transfer process involving an exciton.<sup>1–4</sup> They noted that the enhancement effects were greatest with wide band gap solids and almost

nonexistent with semiconductors. On the other hand, Sagert, Willard, and co-workers attributed the increase in the decomposition of the organics to electron-transfer processes.<sup>5–7</sup> Khare and Johnson used an inorganic matrix system to definitively show that the transfer of energy can depend on the band gap and illustrated the role of excitons in the process.<sup>8</sup>

The first published studies on the radiolysis of adsorbed water were performed on semiconductors and silica gel.<sup>9,10</sup> This work has been followed by other radiolysis studies of water adsorbed on different surfaces and the production of H<sub>2</sub> examined.<sup>11–29</sup> In all cases the yield of H<sub>2</sub> was found to be greater for water on the surface of a solid than for bulk water. It is observed that the type of oxide has a huge effect on H<sub>2</sub> yields. For instance, at about 1  $\mu$ s following the passage of a  $\gamma$ -ray the yield of H<sub>2</sub> is about 0.45 molecule/100 eV of energy absorbed in liquid water.<sup>30</sup> This value is a maximum and is due to intra-track reactions of the water decay products. At longer times the reaction of H<sub>2</sub> with OH radicals leads to a series of reactions to reform water. These back reactions can be suppressed if the H<sub>2</sub> escapes from the liquid water phase, for instance by vaporization into a headspace or purged away by a gas flow. Essentially no H<sub>2</sub> is observed at long times in the radiolysis of closed systems of pure bulk liquid water with  $\gamma$ -rays.<sup>31,32</sup> In contrast, the yield of H<sub>2</sub> from water adsorbed on BeO is as high as 4.4 molecules per 100 eV of energy adsorbed by the entire system.<sup>11</sup>

The observation of an enhanced yield of H<sub>2</sub> in the radiolysis of adsorbed water has led to a number of proposed mechanisms for the transfer of energy from the solid material. Pulsed radiolysis studies on particles adsorbed in water have shown that some of the electrons and holes formed in SiO<sub>2</sub> migrate into the bulk water.<sup>33,34</sup> The recombination of an electron–hole pair on a water molecule at the surface can lead to H<sub>2</sub> production by a dissociative process.<sup>35</sup> Even a single low-energy electron can lead to H<sub>2</sub> formation from water by a dissociative attachment reaction.<sup>36–38</sup> Such a process has been attributed to the observation of H<sub>2</sub> from water on silicon surfaces.<sup>39</sup> Exciton formation

\* Corresponding author.

† Radiation Laboratory, University of Notre Dame.

‡ Chemistry Division, Los Alamos National Laboratory.

and migration to the solid surface is another source of H<sub>2</sub> production. The observations that oxides within a narrow band gap at about 5 eV can lead to a significant increase in H<sub>2</sub> formation suggests that a resonance process is responsible.<sup>28,29</sup> However, not all oxides within this band gap lead to an increase in H<sub>2</sub> yields, and more details are needed. Of course, all of these processes and others can be contributing in various magnitudes to the radiolytic formation of H<sub>2</sub> from adsorbed water.

In this work, the formation of gaseous products from the radiolysis of water adsorbed on CeO<sub>2</sub> and ZrO<sub>2</sub> particles were examined. The irradiations were performed with both  $\gamma$ -rays and 5 MeV helium ions (alpha particles) in order to examine the effect due to the linear energy transfer (LET = stopping power,  $-dE/dx$ ) of the radiation. LET has a significant influence on the production of H<sub>2</sub> in bulk water by varying the concentration of precursors and thereby any second-order reactions involving them.<sup>35</sup> Similar LET effects in solids can lead to more information about the precursors involved in these systems. The adsorption and desorption of water on micron-sized CeO<sub>2</sub> and ZrO<sub>2</sub> particles were examined to determine water loading capacities. H<sub>2</sub> formation was examined as a function of the amount of water adsorbed on the oxide. The experiments give fundamental knowledge related to the mechanism for the formation of H<sub>2</sub> from adsorbed water and provide useful information for the management of nuclear waste materials.

## Experimental Section

Two different lots of CeO<sub>2</sub> (99.9%) and one of ZrO<sub>2</sub> (99.9%) powders were obtained from Alfa Aesar. Particle area measurements were determined on a Quantachrome Autosorb 1 surface area analyzer. This instrument operates by measuring nitrogen adsorption and desorption from the surface at an equilibrium vapor pressure using the BET (Brunauer-Emmet-Teller) method of surface area calculation. Specific areas of the powders were determined to be 2.92 and 4.18 m<sup>2</sup>/g for CeO<sub>2</sub> and 1.99 m<sup>2</sup>/g for ZrO<sub>2</sub>. Particle size measurements were performed on a Horiba LA-900 Laser Scattering Particle Size Distribution Analyzer. This instrument measures the size distribution by number and by volume of the particles suspended in deionized water using the principles of the Mie scattering theory for light. Mean diameters by volume were determined to be 11.47  $\mu$ m (std. dev. 8.92) and 7.62  $\mu$ m (std. dev. 6.35) for CeO<sub>2</sub> and 13.56  $\mu$ m (std. dev. 8.10) for ZrO<sub>2</sub>, respectively. The densities of the oxides are 7.13 g/cm<sup>3</sup> for CeO<sub>2</sub> and 5.6 g/cm<sup>3</sup> for ZrO<sub>2</sub>. Perfect spheres have a specific area equal to  $6/\rho d$ , where  $\rho$  is the oxide density and  $d$  is the diameter. The specific areas predicted are 0.07 and 0.11 m<sup>2</sup>/g for CeO<sub>2</sub> and 0.08 m<sup>2</sup>/g for ZrO<sub>2</sub>, respectively. Since the measured particle specific areas are considerably larger than predicted, the surfaces are not smooth or the particles are clustering.

The oxides were baked at 500 °C for 24 h to remove adsorbed water and any hydrocarbon contaminants. The oxides were cooled in a desiccator, weighted, and placed in a constant humidity chamber. Several different relative humidity chambers were used and each was maintained at a constant humidity using a salt slush.<sup>40</sup> The salts used in this work and their relative humidity at 25 °C are as follow: Mg(NO<sub>3</sub>)<sub>2</sub>, 52.89; NaCl, 75.29; and KCl, 84.34.<sup>41</sup> Water was from a Millipore Milli-Q UV system, and water alone was used to obtain a relative humidity of about 95% (this value was the highest obtainable without air circulation). The oxides were periodically removed from the constant relative humidity chambers and weighted to determine total water adsorbed. The number of water layers was calculated

by assuming the average area of a water molecule to be 0.22 mg/m<sup>2</sup>.<sup>42</sup> Water probably does not adsorb monolayer by monolayer in a nice orderly fashion, but the calculations give useful mean values that can be used as guides.

The heavy ion radiolysis experiments were performed using the facilities of the Nuclear Structure Laboratory of the University of Notre Dame Physics Department. <sup>4</sup>He ions were produced and accelerated using a 10 MeV FN Tandem Van de Graaff. After acceleration, the ions were energy- and charge-state selected magnetically and the energies of the incident ions are known with a precision of about 10 kilovolts. The window assembly was the same as reported earlier and gave a beam diameter of 6.4 mm with a uniform flux across the sample surface.<sup>43,44</sup> Energy loss of the helium ions in passing through all windows was determined from a standard stopping power compilation.<sup>45</sup> The samples were irradiated with completely stripped ions at a charge beam current of about 2 nA. Absolute dosimetry was obtained from the product of the integrated beam current and the particle energy. The ranges of the helium ions ( $\sim 0.013$  mm in both CeO<sub>2</sub> and ZrO<sub>2</sub>) are smaller than the sample thickness so the ions are completely stopped in the sample. The radiation chemical yields represent all processes from the initial particle energy to zero and are therefore track averaged yields. The sample cell ( $\phi \sim 1$  cm, L  $\sim 0.3$  cm) was made of quartz with a thin ( $\sim 4\text{--}6$  mg/cm<sup>2</sup>) mica window epoxied to the front for the beam entrance. Inlet and outlet ports allowed the cell to be purged before and after the irradiation. The use of absolute dosimetry directly gives the radiation chemical yield relative to the energy deposited in the entire sample. However, only a small portion of the total sample is actually irradiated ( $\phi = 6.4$  mm, L  $\sim 0.013$  mm) so the local dose rate is about 2 kGy/s. The particles are small relative to the beam diameter and randomly distributed so partition of energy between the oxide and the adsorbed water is assumed to be equal to the relative electron densities. Irradiations were performed at room temperature (23 °C) and the dose rate was sufficiently small that no macroscopic heating was observed.

Radiolysis with  $\gamma$ -rays was performed using a Gammacell-220 <sup>60</sup>Co source at the Radiation Laboratory of the University of Notre Dame. The dose rate was 202 Gy/min as determined using the Fricke dosimeter.<sup>46</sup> The sample cell was made from a quartz cuvette with inlet and outlet ports for purging the sample before and after irradiation. The same cuvette was used for both dosimetry and sample irradiation. Energy absorbed by the water is directly obtained from the dosimetry and weight of the water in the sample. High Z elements such as cerium and zirconium have a higher photoelectron adsorption cross-section than water. Previous studies with a similar type of source used ionization chambers to determine that the absorbed dose in zirconia is about 10% greater than expected using the Fricke dosimeter.<sup>5,6</sup> Therefore, energy absorption by the total sample was estimated from the weight of the oxide using a 10% higher dose rate than given by the Fricke dosimeter. Total sample weights were 1–2 g. Hydrogen production from cells without oxides, but purged with water-saturated argon, was insignificant (less than the detection limit) when irradiated for times typically used for oxides with adsorbed water. This result is expected since the density and thereby the energy absorption is considerably less. Oxides irradiated without water gave no detectable hydrogen, indicating clean sample surfaces.

Hydrogen was determined using an inline technique with a gas chromatograph and a mass spectrometer. Ultrahigh purity argon was used as the carrier gas with a flow rate of about 50 mL/min. The argon passed through a constant flow regulator,

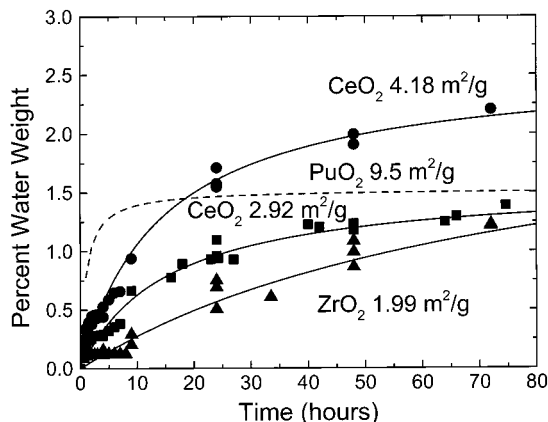


**Figure 1.** Time dependence of the weight of water adsorbed on the oxides at 95% relative humidity: (●) CeO<sub>2</sub> at 4.18 m<sup>2</sup>/g, (■) CeO<sub>2</sub> at 2.92 m<sup>2</sup>/g, (▲) ZrO<sub>2</sub> at 1.99 m<sup>2</sup>/g, this work; (dashed line) PuO<sub>2</sub> at 9.5 m<sup>2</sup>/g, ref 47.

an injection septum, a four-way valve, and into a 3-meter 5× molecular sieve column of an SRI 8610C gas chromatograph with a thermal conductivity detector. Some of the effluent from the thermal conductivity detector was sampled with a quadrupole mass spectrometer (Balzers, QMA140 analyzer with axially mounted secondary electron multiplier) through a capillary tube ( $\phi = 25 \mu\text{m}$ , L = 20 cm). Hydrogen was monitored at mass 2 and oxygen at mass 32. Calibration of the detectors was performed by injecting pure gases with a gas-tight microliter syringe. The estimated error in gas measurement is estimated to be about 5%.

The sample was connected to the gas analysis system using the four-way valve. This loop contained a water bubbler, a relative humidity monitor, and the sample cell. Since the particles took a long time to equilibrate with water, they were first prepared as described above and placed in the constant humidity chambers for several days. The radiolysis procedure was performed by first flowing argon through the sample loop and allowing the relative humidity to equilibrate. This process took about 20 min. The sample was then transferred to the sample cell, purged of air, isolated with the four-way valve and irradiated. Following the irradiation, the four-way valve was opened and the radiolytic gases analyzed. Reweighting of the sample following radiolysis confirmed that the total weight of adsorbed water never varied by more than a few percent.

## Results and Discussion

**Adsorption of Water on the Oxides.** These experiments are designed to compare the radiolysis of adsorbed water with bulk water. Therefore, two critical parameters are required to characterize the adsorbed water: the amount of water on the oxide surface and the rate at which it is adsorbed and desorbed. The significance of the former is obvious since one needs to know how much energy is directly absorbed by the water in these systems. However, the rates of adsorption and desorption must be known in order to determine if equilibrium has been obtained on the oxide surface and to ensure that the water content is not changing during the course of the experiments.

Moisture and any residual hydrocarbons were removed from the oxides by baking. The oxides were then cooled, weighed, and transferred to constant-humidity chambers. Periodically, the oxides were removed from the chambers and reweighed. Figure 1 shows the relative increase in adsorbed water as a function of time for oxides in the 95% relative humidity chamber. The oxides examined here show a slow increase in the amount of

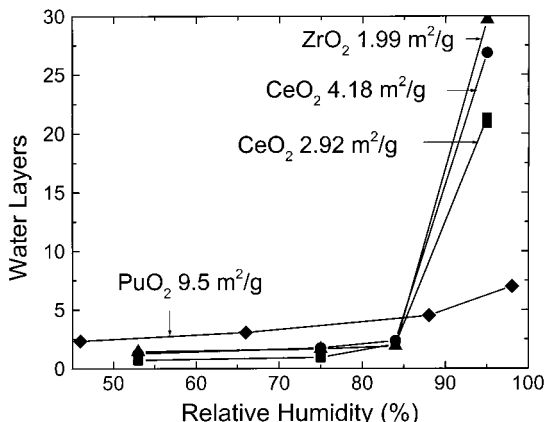


**Figure 2.** Number of water layers as a function of the relative humidity: (●) CeO<sub>2</sub> at 4.18 m<sup>2</sup>/g, (■) CeO<sub>2</sub> at 2.92 m<sup>2</sup>/g, (▲) ZrO<sub>2</sub> at 1.99 m<sup>2</sup>/g, this work; (◆) PuO<sub>2</sub> at 9.5 m<sup>2</sup>/g, ref 47.

water adsorbed with about 15–20 h required for half of the water to adsorb on the ceria. Somewhat more time is required for water to adsorb on the zirconia. The adsorption profiles are very reproducible even after multiple baking and irradiation, which suggests that the surface structures or areas are not permanently affected by these processes. It can be seen that the adsorption profile for PuO<sub>2</sub> rises faster than the oxides examined here.<sup>47</sup> A similar fast rise was observed for PuO<sub>2</sub> at lower relative humidity.<sup>48</sup> The difference could be due to material packing, but variation in the amount of material and the surface exposed to moist air gave no significant difference in the rate of water adsorption. The different adsorption rates are probably real and decrease in the order PuO<sub>2</sub> > CeO<sub>2</sub> > ZrO<sub>2</sub>.

Desorption time profiles of water from the oxide were also determined. It was found that when the saturated oxides were placed in a desiccator (containing anhydrous calcium sulfate) almost all of the water was removed within a few hours. A similar time profile was observed with PuO<sub>2</sub>.<sup>47</sup> Baking was required to remove the final water molecules and return the oxide to its original condition. Half a monolayer of water being present on the surface after baking or in the original sample cannot be ruled out. The comparatively fast desorption rates suggest that at high relative humidity the water is bound by weak physisorption processes. Both adsorption and desorption rates are slow enough that no significant variation in water content with sample manipulation is expected. The relative humidity in the sample loop was always kept equal to or greater than the equilibrium oxide water loading to minimize water loss. In several of the radiolysis studies discussed below, the sample was reanalyzed for water content following radiolysis and no change was found.

The plateau or saturation water content was found for the range of 50 to 95% relative humidity. Lower water loading could not be performed because of the sample size (about 2 g) and the accuracy of the analytical balance. Figure 2 shows the number of water layers at equilibrium as a function of the relative humidity. For conversion to other units, 100% relative humidity at 25 °C corresponds to a vapor pressure of 23.75 mm of Hg or about 3.1% of the atmosphere. The average area of a water molecule was assumed to be 0.22 mg/m<sup>2</sup> following other extensive studies on PuO<sub>2</sub>.<sup>42</sup> This value is not expected to be significantly different for the oxides examined here. It can be seen in Figure 2 that CeO<sub>2</sub> and ZrO<sub>2</sub> have 1 to 2 water layers over the majority of the humidity range. Very high humidity is required for multiple water layers to accumulate on the oxide surfaces. The results for CeO<sub>2</sub> and ZrO<sub>2</sub> are only

slightly different than that for PuO<sub>2</sub>.<sup>47,48</sup> At low relative humidity the water is bound by chemisorption. The number of water layers depends slightly on the particular oxide. Multiple water layers form above about 85% relative humidity, especially for CeO<sub>2</sub> and ZrO<sub>2</sub>. The number of water layers adsorbed does not appear to have a strong dependence on the surface area. This result suggests that variation in surface area is not accompanied by formation of reactive sites that could influence the radiolysis.

**γ-Radiolysis.** The γ-radiolysis of liquid water leads to the production of H<sub>2</sub> by several different mechanisms. Scavenger studies have shown that a major fraction of the total formation of H<sub>2</sub> in the nonhomogeneous chemistry following the passage of ionizing radiation is due to precursors of the hydrated electron.<sup>30</sup> It has been suggested that the mechanism responsible is the dissociative recombination of the water cation and a nonhydrated electron.<sup>30,35</sup> This process competes with electron hydration and water protonation reactions, which occur on the order of a few hundred femtoseconds. Most of the rest of the formation of H<sub>2</sub> is due to reactions of the hydrated electron and H atoms. At about 1 μs following the passage of a γ-ray, the track or string of spurs induced by the radiation has dissipated and the radiolytic products are homogeneously distributed in the medium.<sup>49</sup> Virtually no further radical–radical reactions occur at longer times because their concentrations are too low compared with the molecular products.<sup>31</sup> At long times or under continuous radiation, the yield of H<sub>2</sub> in closed systems decreases due to reactions with OH radicals. Most of the radiolytic products in the radiolysis of pure liquid water with γ-rays are converted back to water.<sup>31</sup> In practice, dissolved oxygen and other impurities scavenge the radical species before they convert much of the molecular products back to water. Gaseous products can also escape into any available headspace, which would effectively keep their concentrations in the liquid water lower than in closed systems. Throughout this work it will be assumed that the yield of H<sub>2</sub> in the radiolysis of bulk water is the yield at about 1 μs. In the γ-radiolysis of water, the microsecond yield of H<sub>2</sub> is about 0.45 molecules/100 eV of energy absorbed.<sup>30</sup> No other gaseous products have been reported in the γ-radiolysis of liquid water in closed systems. The main oxidizing product in the γ-radiolysis of liquid water is not O<sub>2</sub>, but H<sub>2</sub>O<sub>2</sub>.<sup>31,49</sup>

Reported yields of H<sub>2</sub> in the radiolysis of gaseous water vary by a factor of 10<sup>4</sup> due to impurities, wall effects, dose rates, etc.<sup>50</sup> However, the H<sub>2</sub> yield in a properly scavenged system is also 0.45 molecule/100 eV, similar to that in the liquid.<sup>50</sup> The radiolysis of one or two layers of adsorbed water probably does not resemble that of bulk liquid water because electrons cannot hydrate and desorption of products can readily occur. However, these water molecules also do not behave like gaseous water since they are not isolated from other molecules and collisional effects can occur. The experiments reported here vary from a monolayer of water to more than twenty, where bulk water properties are expected to occur. Most of the discussion will compare the radiolytic response of adsorbed water to bulk liquid water, and variations in mechanisms may occur at low water coverage.

The production of H<sub>2</sub> from the radiolysis of water adsorbed on the surface of oxides was examined as a function of the energy absorbed in the water layer. Any significant deviation in yields would be due to the heterogeneous effect of the oxide boundary. The radiation chemical yield, *G*-value (units of molecules/100 eV), for the formation of H<sub>2</sub> from water in equilibrium at 95% relative humidity on CeO<sub>2</sub> is about 1.4 when determined with respect to the amount of adsorbed water. The

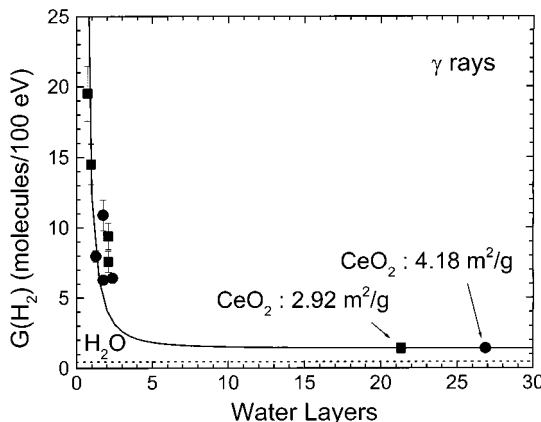


**Figure 3.** Production of H<sub>2</sub> relative to the amount of energy directly deposited by γ-rays in the water adsorbed on CeO<sub>2</sub> as a function of the number of water layers: (●) CeO<sub>2</sub> at 4.18 m<sup>2</sup>/g, (■) CeO<sub>2</sub> at 2.92 m<sup>2</sup>/g. The dashed line is the limiting yield for liquid water.

corresponding value for ZrO<sub>2</sub> is 6.9 molecules/100 eV of energy deposited directly in the adsorbed water. Most of the other heterogeneous studies on H<sub>2</sub> formation also find an increase in its yield. Clearly, the increase in H<sub>2</sub> formation can be significant at heterogeneous interfaces. The enhanced yield of H<sub>2</sub> is solely due to a radiolytic effect and not catalytic. Successive irradiations of the same dose produced identical amounts of H<sub>2</sub> suggesting the yield is linear up to doses of about 50 kGy. Adsorbed water left in contact with the oxide for extended periods without being irradiated did not produce any gaseous product, even after the oxide had been irradiated.

Only H<sub>2</sub> was observed in the γ-radiolysis of CeO<sub>2</sub> and ZrO<sub>2</sub>. Any O<sub>2</sub> produced in the radiolysis of these oxides has a yield at least an order of magnitude less than that of H<sub>2</sub>. Similar results are found with wet UO<sub>2</sub>.<sup>51</sup> The lack of O<sub>2</sub> production is observed at all water loadings, to be discussed below. The radiolysis of adsorbed water is obviously much different than its UV photolysis where near stoichiometric production of H<sub>2</sub> and O<sub>2</sub> is found from water on ZrO<sub>2</sub>.<sup>52</sup> The stable oxidizing product in radiolysis could be H<sub>2</sub>O<sub>2</sub> as observed in bulk water. However, it is hard to imagine H<sub>2</sub>O<sub>2</sub> being solvated in the few water layers available. The peroxide could be chemisorbed intact or decomposed to OH radicals that are then chemisorbed to the oxide surface. The photochemistry of H<sub>2</sub>O<sub>2</sub> in solid argon suggests the scheme H<sub>2</sub>O<sub>2</sub> ↔ H<sub>2</sub>O<sub>2</sub> → 2OH exists, which may be occurring in the thin water layer due to the stabilizing effect of the radicals at the oxide surface.<sup>53</sup> The photochemical and the thermal decomposition of gaseous H<sub>2</sub>O<sub>2</sub> is not thought to lead to the production O<sub>2</sub>, but rather two OH radicals.<sup>54–56</sup> The results here also suggest that if H<sub>2</sub>O<sub>2</sub> is formed in the water layers it does not decompose to O<sub>2</sub>. Studies on the low-energy electron radiolysis of ice find the O atom and this species could be occurring in the present situation.<sup>57</sup> It has been reported that the self-radiolysis of water adsorbed on PuO<sub>2</sub> leads to the oxidation of Pu(IV) to Pu(VI).<sup>58</sup> There have also been several studies suggesting the oxidation of UO<sub>2</sub> to either U<sub>3</sub>O<sub>7</sub> or U<sub>3</sub>O<sub>8</sub> following α- or γ-radiolysis of water in contact with nuclear fuel.<sup>51,59–63</sup> This oxidation could be responsible for the incorporation of oxygen into the bulk oxide. None of these processes can be ruled out for the oxides examined here and further studies on the material science of these systems are required.

The dependence of H<sub>2</sub> on the percent water loading was determined in the γ-radiolysis of CeO<sub>2</sub> and ZrO<sub>2</sub>. Figure 3 shows the results for H<sub>2</sub> yields as a function of the number of water layers in the γ-radiolysis of CeO<sub>2</sub>. It was found that the H<sub>2</sub> yield

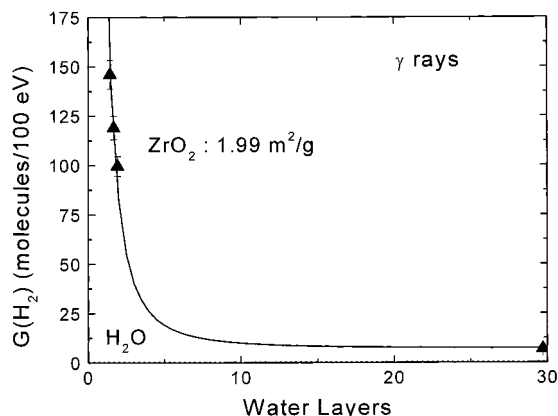


**Figure 4.** Production of  $\text{H}_2$  relative to the amount of energy directly deposited by  $\gamma$ -rays in the water adsorbed on  $\text{ZrO}_2$  ( $1.99 \text{ m}^2/\text{g}$ ) as a function of the number of water layers. The dashed line is the limiting yield for liquid water.

is as high as 20 molecules/100 eV for the single water layer corresponding to about 50% relative humidity. This value is a factor of 40 greater than that found in bulk water. There appears to be no difference due to the oxide surface area except for the amount of water loading. Figure 4 shows similar results for the  $\gamma$ -radiolysis of  $\text{ZrO}_2$ . For this oxide, the maximum yield at 1–2 layers of water is about 150 molecules/100 eV or more than 2 orders of magnitude larger than observed in bulk water. It is obvious that some mechanism can lead to a significant increase in  $\text{H}_2$  yields.

Several processes may be contributing to the increased yield of  $\text{H}_2$  with decreasing water layers such as steric or other surface effects. However, it is equally likely that one is mainly observing a “dilution” effect as the number of water layers increases. Even the earliest studies on heterogeneous effects in radiolysis suggest that energy is being transferred from the solid to the adsorbed layer.<sup>1–8</sup> Recent studies on the pulsed radiolysis of oxide suspensions show an excess of electrons and holes in bulk water, which is attributed to migration of species from the oxide surface.<sup>33,34</sup> In all of the experiments performed here the oxide is the dominant material being irradiated. Energy deposited in the oxide that is transferred to the adsorbed water layer can be available to produce  $\text{H}_2$ . An increase in the number of water layers leads to an effective decrease in  $\text{H}_2$  yield when the direct energy deposition is determined relative to the number of water layers, and the fraction of energy escaping the oxide is constant.

It is somewhat easier to elucidate the process of energy transfer by examining the yields relative to the total energy loss in the oxide and water system. The observed  $\text{H}_2$  yields with respect to the energy absorbed by the total system is shown in Figure 5 as a function of the water weight percent on the oxides. There is a smaller dependence of  $\text{H}_2$  yield on the amount of water present on  $\text{ZrO}_2$  than for  $\text{CeO}_2$ . However, this dependence is not negligible, especially for  $\text{CeO}_2$ . Extrapolation of the linear fits in Figure 5 to 100% water leads to  $G$ -values of  $\text{H}_2$  of 0.28 and 1.04 for  $\text{ZrO}_2$  and  $\text{CeO}_2$ , respectively. Either the surface is affecting the yield of  $\text{H}_2$  from that of normal bulk water, or more likely, the range of water loading examined is too small to accurately predict the true functional dependence. If one assumes that the yield of  $\text{H}_2$  in adsorbed water is the same as bulk water (0.45 molecule/100 eV) then the amount of energy transferring from the oxide to the water is about 4% for  $\text{CeO}_2$  and 18% for  $\text{ZrO}_2$ . This approach is very simplistic since it assumes direct energy transfer without concerning the mechanism for the transfer. Furthermore, the maximum  $\text{H}_2$  yield would

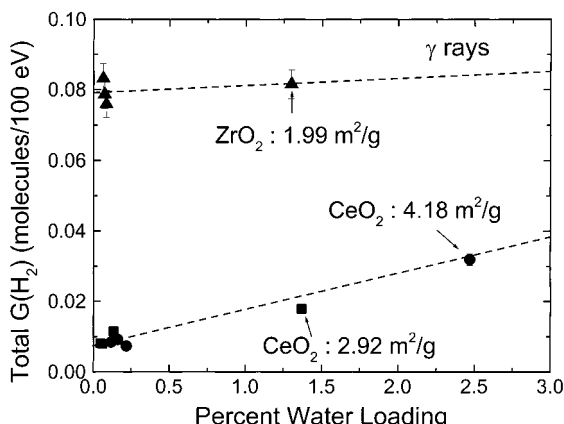


**Figure 5.** Production of  $\text{H}_2$  relative to the amount of total energy deposited by  $\gamma$ -rays as a function of the weight percent of water on the oxides: (●)  $\text{CeO}_2$  at  $4.18 \text{ m}^2/\text{g}$ , (■)  $\text{CeO}_2$  at  $2.92 \text{ m}^2/\text{g}$ , (▲)  $\text{ZrO}_2$  at  $1.99 \text{ m}^2/\text{g}$ .

be 0.45 when all of the energy is transferred to the water layer. Yields of  $\text{H}_2$  with respect to the total energy deposited in the system are as high as 0.9, 1.3, 1.4, and 4.4 molecules of  $\text{H}_2$  per 100 eV for  $\text{Al}_2\text{O}_3$ ,  $\text{Er}_2\text{O}_3$ ,  $\text{La}_2\text{O}_3$ , and  $\text{BeO}$ , respectively.<sup>13</sup> The mechanisms responsible for energy transfer from the oxide and for  $\text{H}_2$  production are obviously important when such high yields are observed.

Recent work on  $\text{H}_2$  production from water adsorbed on a number of oxides shows that the nature of the oxide is extremely important.<sup>17,28,29</sup> Various oxides can be classified according to whether they increase, decrease, or have no effect on  $\text{H}_2$  yields compared to that found in the water alone. A strong argument has been made that some, but not all, oxides with a band gap at about 5 eV are able to lead to an increase in  $\text{H}_2$  yields.<sup>29</sup> The proposed mechanism is the formation and migration of an exciton in the bulk oxide. This exciton couples in a resonant process with the adsorbed water to give  $\text{H}_2$ . Radiation chemical yields were not determined in this work, but there was a substantial increase in  $\text{H}_2$  production from water on  $\text{ZrO}_2$  as compared to  $\text{CeO}_2$ . This result is similar to the present observations. Because of the nature of the materials it is hard to determine the band gaps of actinide oxides present in nuclear wastes such as  $\text{PuO}_2$  or  $\text{UO}_2$ . Some literature reports suggest that the band gaps in these materials are more similar to  $\text{CeO}_2$  than to  $\text{ZrO}_2$ .<sup>64–69</sup>

**Heavy Ion Radiolysis of Water Adsorbed on Oxides.** The radiolysis of materials with heavy ions leads to an increase in the local density of reactive species in the nonhomogeneous region making up the particle track. The local track structure determines the spatial distribution of reactive species and thereby the kinetics. No one parameter, such as particle energy or velocity, determines the track structure, but to a first approximation, the concentrations of reactive species can be related to the LET of the particle. Higher concentrations of reactive species lead to an increase in second-order reactions without affecting first-order ones. Therefore, heavy ion radiolysis can be used as an effective probe of the kinetics leading to the observed results. Helium ions at 5 MeV were used because their track average LET is high (about 410 eV/nm for both oxides) and the results with  $\alpha$ -particle radiolysis are of immense practical importance.

The results for the 5 MeV helium ion radiolysis of water on  $\text{CeO}_2$  and  $\text{ZrO}_2$  are shown in Figure 6.  $\text{H}_2$  yields with respect to the total energy deposited in the system are presented as a function of the percent weight of water loading. In all cases,

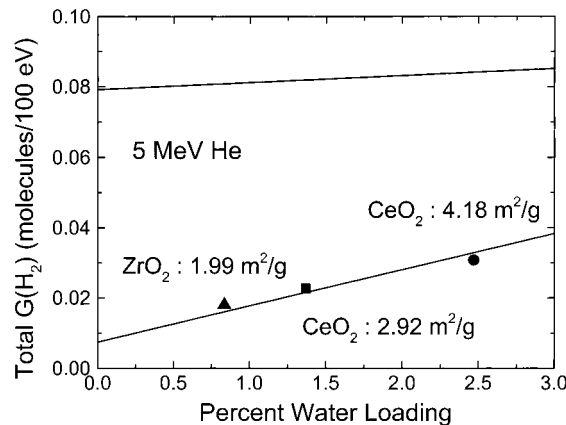


**Figure 6.** Production of H<sub>2</sub> relative to the amount of total energy deposited by 5 MeV <sup>4</sup>He ions as a function of the weight percent of water on the oxides: (●) CeO<sub>2</sub> at 4.18 m<sup>2</sup>/g, (■) CeO<sub>2</sub> at 2.92 m<sup>2</sup>/g, (▲) ZrO<sub>2</sub> at 1.99 m<sup>2</sup>/g. The solid lines are the  $\gamma$ -radiolysis results from Figure 5.

the water is in equilibrium at 95% relative humidity. The solid lines in the figure are the same lines as in Figure 5 and are obtained by a linear fit of the  $\gamma$ -radiolysis results for each oxide. It can be seen that there is virtually no difference between the H<sub>2</sub> yields in the  $\gamma$ -radiolysis or the helium ion radiolysis of water adsorbed on CeO<sub>2</sub>. On the other hand, the H<sub>2</sub> yields for ZrO<sub>2</sub> show a marked decrease in helium ion radiolysis compared to the  $\gamma$ -radiolysis. It appears that the helium ion radiolysis gives similar results regardless of the type of particle. There is not enough data to completely substantiate this claim, and more experiments will be performed in the future using oxides of different surface area. Experiments with helium ions could not be performed on the present oxides at lower water content. A slight lowering of the relative humidity from 95 to 85% gives a large decrease from over 20 water layers to 1 or 2, see Figure 2. The local dose of the helium ions is so high that 1 or 2 water layers are not sufficient to form observable H<sub>2</sub> before all the water in the radiation field is completely destroyed. Reduction of the beam current by an order of magnitude gave no observable change in the radiolytic yield. Migration of water from particle to particle or readsorption from the gas phase is too slow on the experimental irradiation time scale.

It is well-known that radiation induces point defects in oxides.<sup>70</sup> Frenkel defects due to the displacement of an atom to form an interstitial/vacancy pair are especially common with heavy ions because of the large relative momentum transfer possible in nuclear collisions.<sup>71</sup> The local density of Frenkel defects in a heavy ion track is much greater than found in  $\gamma$ -radiolysis and it has been proposed that in some oxides this high density of defects leads to considerable self-trapping of excitons.<sup>72</sup> If the main carrier of energy through the particle is due to excitons as previously proposed,<sup>28,29</sup> then a decrease in H<sub>2</sub> yields is expected with heavy ion radiolysis. The near similarity in yield for helium ions and  $\gamma$ -rays suggest that another minor mode of energy transfer from the particle to the water layer is also possible. This near-surface effect is probably due to the escape of electrons and holes as observed in particle suspensions.<sup>33,34</sup> The ranges of electrons and holes are relatively short compared to the size of the particles examined here so they predominate as a near-surface effect when excitation formation or transport is diminished. Further heavy ion radiolysis studies with a wider range of particle sizes and surface areas will hopefully elucidate more characteristics of the energy carriers in simple oxides.

## Conclusions

These experiments have examined the production of H<sub>2</sub> in the radiolysis of water adsorbed on micron-sized particles of CeO<sub>2</sub> and ZrO<sub>2</sub>. Radiation chemical yields of H<sub>2</sub> increase substantially with decreasing number of adsorbed water layers when the yield is determined with respect to the energy deposited directly by  $\gamma$ -rays to the water. These yields reached values of 20 molecules of H<sub>2</sub> per 100 eV for one water layer on CeO<sub>2</sub> and up to 150 molecules/100 eV for two water layers on ZrO<sub>2</sub>. The corresponding yield for H<sub>2</sub> in liquid and gaseous water is only about 0.45 molecule/100 eV. The yields of H<sub>2</sub> determined with respect to the total energy deposited in both the oxide and water were found to have a smaller, but observable, dependence on the amount of water adsorbed. Radiolysis of ZrO<sub>2</sub> with  $\gamma$ -rays produced about 5 times more H<sub>2</sub> than CeO<sub>2</sub> for the equivalent amount of water adsorbed. In all of the experiments, the O<sub>2</sub> yield was at least an order of magnitude less than that of H<sub>2</sub>. These experiments cannot determine where the oxygen is incorporated or its state. The results suggest that the increase in H<sub>2</sub> production is due to the transfer of energy, possibly by an exciton, from the oxide to the water. The yield of H<sub>2</sub> in the 5 MeV helium ion radiolysis of water on CeO<sub>2</sub> is the same as with  $\gamma$ -rays, but the results with ZrO<sub>2</sub> are substantially lower. A change in LET affects second-order reactions so these results suggest that such processes in the bulk oxide can quench the precursor responsible for the large H<sub>2</sub> yields from water on ZrO<sub>2</sub>. The H<sub>2</sub> yields with helium ion radiolysis seem to be nearly independent of the type of oxide, but further studies will be required to substantiate this claim.

**Acknowledgment.** The authors thank Professor J. J. Kolata for making the facilities of the Notre Dame Nuclear Structure Laboratory available. The latter is funded by the National Science Foundation. The authors also thank Julie Bremser and her team at LANL for the surface area and particle diameter measurements and Mark Paffett of LANL for valuable technical discussions and providing some of the oxides. The 94-1 Program from Los Alamos National Laboratory of the U.S. Department of Energy supported the work described herein. The DOE Nuclear Materials Stewardship Program, through the Nuclear Materials Project Office in the Albuquerque Operations Center, supports the 94-1 Program. This contribution is NDRL-4320 from the Notre Dame Radiation Laboratory, which is supported by the Office of Basic Energy Sciences of the U.S. Department of Energy.

## References and Notes

- (1) Caffrey, J. M., Jr.; Allen, A. O. *J. Phys. Chem.* **1958**, 62, 33.
- (2) Sutherland, J. W.; Allen, A. O. *J. Am. Chem. Soc.* **1961**, 83, 1040.
- (3) Rabe, J. G.; Rabe, B.; Allen, A. O. *J. Am. Chem. Soc.* **1964**, 86, 3887.
- (4) Rabe, J. G.; Rabe, B.; Allen, A. O. *J. Phys. Chem.* **1966**, 70, 1098.
- (5) Sagert, N. H.; Dyne, P. J. *Can. J. Chem.* **1967**, 45, 615.
- (6) Sagert, N. H.; Robinson, R. W. *Can. J. Chem.* **1968**, 46, 2075.
- (7) Wong, P. K.; Willard, J. E. *J. Phys. Chem.* **1968**, 72, 2623.
- (8) Khare, M.; Johnson, E. R. *J. Phys. Chem.* **1970**, 74, 4085.
- (9) Krylova, Z. L.; Dolin, P. I. *Kinetics Catalysis (USSR) (English Transl.)* **1966**, 7, 840.
- (10) Bubyreva, N. S.; Dolin, P. I.; Kononovich, A. A.; Rozenblyum, N. D. *Kinet. Catal. (USSR) (English Transl.)* **1966**, 7, 846.
- (11) Garibov, A. A.; Melikzade, M. M.; Bakirov, M. Ya.; Ramazanova, M. Kh. *High Energy Chem.* **1982**, 16, 101.
- (12) Rustamov, V. R.; Bugaenko, L. T.; Kurbanov, M. A.; Kerimov, V. K. *High Energy Chem.* **1982**, 16, 148.
- (13) Garibov, A. A.; Melikzade, M. M.; Bakirov, M. Ya.; Ramazanova, M. Kh. *High Energy Chem.* **1982**, 16, 177.

- (14) Garibov, A. A. *Proceedings of the Fifth Symposium on Radiation Chemistry*; Dobo, J., Hedvig, P., Schiller, R., Eds.; Akademiai Kiado: Budapest 1983; p 377.
- (15) Garibov, A. A.; Bakirov, M. Ya.; Velibekova, G. Z.; Elchiev, Ya. M. *High Energy Chem.* **1984**, *18*, 398.
- (16) Nechaev, A. *Radiat. Phys. Chem.* **1986**, *28*, 433.
- (17) Aleksandrov, A. B.; Gusev, A. L.; Petrik, N. G. *Russ. J. Phys. Chem.* **1987**, *61*, 102.
- (18) Garibov, A. A.; Gezalov, Kh. B.; Velibekova, G. Z.; Khudiev, A. T.; Ramazanova, M. Kh.; Kasumov, R. D.; Agaev, T. N.; Gasanov, A. M. *High Energy Chem.* **1987**, *21*, 416.
- (19) Nakashima, M.; Tachikawa, E. *J. Nucl. Sci. Technol.* **1987**, *24*, 41.
- (20) Gezalov, K. B.; Gasanov, A. M.; Garibov, A. A.; Abdullayeva, K. I. *Radiat. Phys. Chem.* **1988**, *32*, 615.
- (21) Garibov, A. A.; Velibekova, G. Z.; Kasumov, R. D.; Gezalov, Kh. B.; Agaev, T. N. *High Energy Chem.* **1990**, *24*, 174.
- (22) Garibov, A. A.; Parmon, V. N.; Agaev, T. N.; Kasumov, R. D. *High Energy Chem.* **1991**, *25*, 86.
- (23) Garibov, A. A.; Agaev, T. N.; Kasumov, R. D. *High Energy Chem.* **1991**, *25*, 337.
- (24) Aleksandrov, A. B.; Bychkov, A. Yu.; Vall A. I.; Petrik, N. G.; Sedov, V. M. *Russ. J. Phys. Chem.* **1991**, *65*, 847.
- (25) Garibov, A. A.; Velibekova, G. Z.; Agaev, T. N.; Dzhafarov, Ya. D.; Gadzhieva, N. N. *High Energy Chem.* **1992**, *26*, 184.
- (26) Nakashima, M.; Aratono, Y. *Radiat. Phys. Chem.* **1993**, *41*, 461.
- (27) Nakashima, M.; Masaki, N. M. *Radiat. Phys. Chem.* **1996**, *47*, 241.
- (28) Petrik, N. G.; Alexandrov, A. B.; Orlando, T. M.; Vall, A. I. *Trans. Am. Nucl. Soc.* **1999**, *81*, 101.
- (29) Petrik, N. G.; Alexandrov, A. B.; Vall, A. I. *J. Phys. Chem. B* **2001**, *105*, 5935.
- (30) Pastina, B.; LaVerne, J. A.; Pimblott, S. M. *J. Phys. Chem. A* **1999**, *103*, 5841.
- (31) Pastina, B.; LaVerne, J. A. *J. Phys. Chem. A* **2001**, *105*, 9316.
- (32) Allen, A. O. *The Radiation Chemistry of Water and Aqueous Solutions*; Van Nostrand: New York, 1961.
- (33) Schatz, T.; Cook, A. R.; Meisel, D. *J. Phys. Chem. B* **1998**, *102*, 7225.
- (34) Dimitrijevic, N. M.; Henglein, A.; Meisel, D. *J. Phys. Chem. B* **1999**, *103*, 7073.
- (35) LaVerne, J. A.; Pimblott, S. M. *J. Phys. Chem. A* **2000**, *104*, 9820.
- (36) Rowntree, P.; Parenteau, L.; Sanche, L. *J. Chem. Phys.* **1991**, *94*, 8570.
- (37) Kimmel, G. A.; Orlando, T. M.; Vezina, C.; Sanche, L. *J. Chem. Phys.* **1994**, *101*, 3282.
- (38) Cobut, V.; Jay-Gerin, J.-P.; Frongillo, Y.; Patau, J. P. *Radiat. Phys. Chem.* **1996**, *47*, 247.
- (39) Klyachko, D. V.; Rowntree, P.; Sanche, L. *Surf. Sci.* **1997**, *389*, 29.
- (40) American Society for Testing Materials, E104–85, 1996. Standard Practice for Maintaining Constant Relative Humidity by Means of Aqueous Solutions.
- (41) *CRC Handbook of Chemistry and Physics*, 77th ed.; Chemical Rubber Company: Boca Raton, FL, 1996–1997; pp 15–24.
- (42) Haschke, J. M.; Ricketts, T. E. *J. Alloy Compd.* **1997**, *252*, 148.
- (43) LaVerne, J. A.; Schuler, R. H. *J. Phys. Chem.* **1987**, *91*, 5770.
- (44) LaVerne, J. A.; Schuler, R. H. *J. Phys. Chem.* **1987**, *91*, 6560.
- (45) Ziegler, J. F.; Biersack, J. P.; Littmark, U. *The Stopping Power and Range of Ions in Solids*; Pergamon: New York, 1985.
- (46) Pastina, B.; LaVerne, J. A. *J. Phys. Chem. A* **1999**, *103*, 1592.
- (47) Benhamou, A.; Beraud, J. P. *Analisis* **1980**, *8*, 376.
- (48) Haschke, J. M.; Ricketts, T. E. *J. Alloys Compd.* **1997**, *252*, 148.
- (49) LaVerne, J. A. *Radiat. Res.* **2000**, *153*, 487.
- (50) Dixon, R. S. *Radiat. Res. Rev.* **1970**, *2*, 237.
- (51) Eriksen, T. E.; Eklund, U.-B.; Werme, L.; Bruno, J. *J. Nucl. Mater.* **1995**, *227*, 76.
- (52) Sayama, K.; Arakawa, H. *J. Phys. Chem.* **1993**, *97*, 531.
- (53) Khriahtchev, L.; Pettersson, M.; Tuominen, S.; Rasanen, M. *J. Chem. Phys.* **1997**, *107*, 7252.
- (54) Bohn, B.; Zetzs, C. *J. Phys. Chem. A* **1997**, *101*, 1488.
- (55) Takagi, J.; Ishigure, K. *Nucl. Sci. Eng.* **1985**, *89*, 177.
- (56) Einschlag, F. G.; Feliz, M. R.; Capparelli, A. L. *J. Photochem. Photobiol.* **1997**, *110*, 235.
- (57) Kimmel, G. A.; Orlando, T. M. *Phys. Rev. Lett.* **1995**, *75*, 2606.
- (58) Haschke, J. M.; Allen, T. H.; Morales, L. A. *Science* **2000**, *287*, 285.
- (59) Christensen, H.; Sunder, S.; Shoesmith, D. W. *J. Alloys Compd.* **1996**, *213/214*, 93.
- (60) Sunder, S.; Miller, N. H. *J. Nucl. Mater.* **1996**, *231*, 121.
- (61) Taylor, P.; Hocking, W. H.; Johnson, L. H.; McEachern, R. J.; Sunder, S. *Nucl. Technol.* **1996**, *116*, 222.
- (62) Wronkiewicz, D. J.; Bates, J. K.; Wolf, S. F.; Buck, E. C. *J. Nucl. Mater.* **1996**, *238*, 78.
- (63) Sunder, S.; Shoesmith, D. W.; Miller, N. H. *J. Nucl. Mater.* **1997**, *244*, 66.
- (64) Strehlow, W. H.; Cook, E. L. *J. Phys. Chem. Ref. Data* **1973**, *2*, 163.
- (65) Young R. A. *J. Nucl. Mater.* **1979**, *87*, 283.
- (66) Gubanov, V. B.; Rosen, A.; Ellis, D. E. *J. Phys. Chem. Solids* **1979**, *40*, 17.
- (67) Naito, K.; Tsuji, T.; Ouchi, K.; Yahata, T.; Yamashita, T.; Tagawa, H. *J. Nucl. Mater.* **1980**, *95*, 181.
- (68) Winter, P. W. *J. Nucl. Mater.* **1989**, *161*, 38.
- (69) Dudarev, S. L.; Castell, M. R.; Botton, G. A.; Savrasov, S. Y.; Muggelberg, C.; Briggs, G. A. D.; Sutton, A. P.; Goddard, D. T. *Micron* **2000**, *31*, 363.
- (70) Kotomin, E. A.; Popov, A. I. *Nucl. Inst. Methods Phys. Res. B* **1998**, *141*, 1.
- (71) Chadderton, L. T. *Radiation Damage in Crystals*; John Wiley & Sons: New York, 1965.
- (72) Itoh, N. *Nucl. Inst. Methods Phys. Res. B* **1996**, *116*, 33.